Author/s:
Czuba-Wojnilowicz, E;Klemm, V;Cortez-Jugo, C;Turville, S;Aggarwal, A;Caruso, F;Kelleher, AD;Ahlenstiel, CL

Title:
Layer-by-Layer Particles Deliver Epigenetic Silencing siRNA to HIV-1 Latent Reservoir Cell Types

Date:
2023-04-03

Citation:
Czuba-Wojnilowicz, E., Klemm, V., Cortez-Jugo, C., Turville, S., Aggarwal, A., Caruso, F., Kelleher, A. D. & Ahlenstiel, C. L. (2023). Layer-by-Layer Particles Deliver Epigenetic Silencing siRNA to HIV-1 Latent Reservoir Cell Types. Molecular Pharmaceutics, 20 (4), pp.2039-2052. https://doi.org/10.1021/acs.molpharmaceut.2c01030.

Layer-by-Layer Particles Deliver Epigenetic Silencing siRNA to HIV-1 Latent Reservoir Cell Types

Journal:	*Molecular Pharmaceutics*
Manuscript ID	mp-2022-01030y.R2
Manuscript Type:	Article
Date Submitted by the Author:	12-Feb-2023
Complete List of Authors:	Czuba-Wojnilowicz, Ewa; University of Melbourne, Chemical and Biomolecular Engineering Klemm, Vera; University of New South Wales Cortez-Jugo, Christina; University of Melbourne, Chemical and Biomolecular Engineering Turville, Stuart; University of New South Wales Aggarwal, Anupriya; University of New South Wales Caruso, Frank; University of Melbourne, Chemical and Biomolecular Engineering; Chemistry of Materials, Chemical and Biomolecular Engineering Kelleher, Anthony; University of New South Wales Ahlenstiel, Chantelle; University of New South Wales

Layer-by-Layer Particles Deliver Epigenetic Silencing siRNA to HIV-1 Latent Reservoir Cell Types

Ewa Czuba-Wojnilowicz,[1‡] Vera Klemm,[2‡] Christina Cortez-Jugo,[1] Stuart Turville,[2] Anupriya Aggarwal,[2] Frank Caruso,[1] Anthony D. Kelleher,[2,3] and Chantelle L. Ahlenstiel[2,3]**

[1]Department of Chemical Engineering, The University of Melbourne, Parkville, Victoria 3010, Australia

[2]Kirby Institute, UNSW Medicine, Sydney, New South Wales 2052, Australia

[3]UNSW RNA Institute, UNSW Sydney, New South Wales, 2052, Australia

*Corresponding authors. E-mail: cahlenstiel@kirby.unsw.edu.au; ccortez@unimelb.edu.au

‡Both authors contributed equally

KEYWORDS: Layer-by-layer; poly-L-arginine; siRNA delivery; HIV-1 latent reservoir; epigenetic silencing

ABSTRACT

For over two decades, nanomaterials have been employed to facilitate intracellular delivery of small interfering RNA (siRNA), both *in vitro* and *in vivo,* to induce post-transcriptional gene silencing (PTGS) via RNA interference. Besides PTGS, siRNAs are also capable of

transcriptional gene silencing (TGS) or epigenetic silencing, which targets the gene promoter in the nucleus and prevents transcription via repressive epigenetic modifications. However, silencing efficiency is hampered by poor intracellular and nuclear delivery. Here, polyarginine-terminated multilayered particles are reported as a versatile system for the delivery of TGS-inducing siRNA to potently suppress virus transcription in HIV-infected cells. siRNA is complexed with multilayered particles formed by layer-by-layer assembly of poly(styrene sulfonate) and poly(arginine) and incubated with HIV-infected cell types, including primary cells. Using deconvolution microscopy, uptake of fluorescently labeled siRNA is observed in nuclei of HIV-1 infected cells. Viral RNA and protein are measured to confirm functional virus silencing from siRNA delivered using particles 16 days post-treatment. This work extends conventional particle-enabled PTGS siRNA delivery to the TGS pathway and paves the way for future studies on particle-delivered siRNA for efficient TGS of various diseases and infections, including HIV.

INTRODUCTION

Small interfering RNA (siRNA) can alter the expression of target genes via gene knockdown or silencing in a pathway called RNA interference (RNAi). RNAi can occur via post-transcriptional gene silencing (PTGS) or via transcriptional gene silencing (TGS) (Figure 1). PTGS occurs when siRNA, complexed with Argonaute 2 (Ago2) in the RNA-induced silencing complex (RISC), binds to its complementary target messenger RNA (mRNA) sequence predominantly in the cytoplasm, resulting in mRNA cleavage and gene silencing.[1, 2] TGS occurs when siRNA enters the nucleus and together with Argonaute 1 (Ago1) in the RNA-induced initiation of transcriptional silencing (RITS) complex binds to the target DNA sequence in the genome and triggers chromatin compaction, resulting in silencing of the gene promoter at the level of transcription, hence the name transcriptional gene silencing.[3,4] In both PTGS and TGS, effective gene silencing is largely hampered by intracellular delivery of siRNA

inside cells (predominantly in the cytoplasm for PTGS and nucleus for TGS) due to poor transport across membranes, limited endosomal escape and nuclease degradation of siRNA.

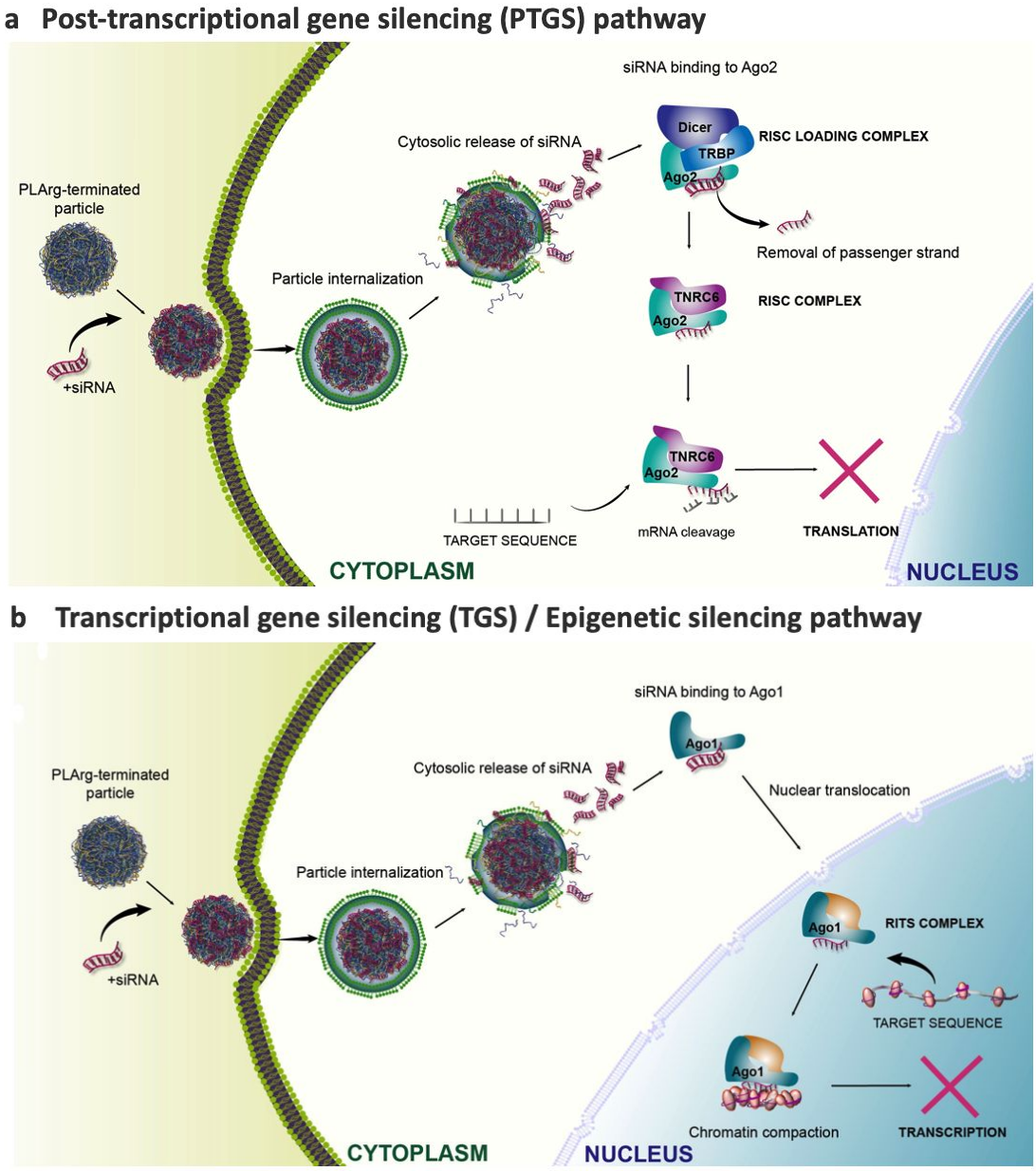

Figure 1. Particle-mediated delivery of siRNA for gene silencing. (a) Upon particle internalization, the released siRNA binds to Ago2 to form the RISC complex, which facilitates removal of the siRNA passenger strand. The RISC-loaded guide strand binds to its complementary sequence of target mRNA in the cytosol, leading to mRNA cleavage and lack of translation of mRNA transcript into protein via PTGS. (b) In TGS, siRNA requires nuclear translocation from the cytosol to target the genomic sequence. Released siRNA in the cytoplasm binds to Ago1, transporting the siRNA through the nuclear membrane, where the

RITS complex is formed, and the passenger strand is removed. In the nucleus, the RITS-loaded guide strand binds to its complementary sequence in the genome and induces epigenetic changes, preventing transcription of DNA into mRNA. Created with BioRender.com.

Significant advances have been made in nanotechnology and chemistry in RNAi drug (siRNA) delivery for PTGS, including encapsulation within lipid- and polymer-based particles, and chemical modification to enhance nuclease resistance for *in vivo* delivery.[2] This is demonstrated in the United States Food and Drug Administration (FDA) approval of four RNAi PTGS-inducing siRNA products: i) patisiran (ONPATRRO) in 2018, which is encapsulated in a lipid nanoparticle and approved to treat hereditary transthyretin-mediated amyloidosis; ii) givosiran (GIVLAARI) in 2019, a N-acetylgalactosamine (GalNAc)-siRNA conjugate used to treat acute hepatic porphyria; iii) lumasiran (OXLUMO) in 2020, also a GalNAc-siRNA conjugate approved to treat primary hyperoxaluria type 1; and iv) inclisiran in 2022, another GalNAc-siRNA conjugate approved to treat hypercholesterolaemia and atherosclerotic cardiovascular disease. Several siRNA products are currently in phase 3 trials and the rapid development and approval of COVID-19 disease targeting mRNA in the Pfizer and Moderna lipid nanoparticle vaccines highlights the rapidly expanding field of RNA therapeutics. However, in stark contrast to PTGS-inducing siRNAs, which only need to reach the cytoplasm, the use of particles to facilitate entry of siRNA into the nucleus to mediate epigenetic silencing via TGS has not been reported.

Epigenetic silencing using siRNA has been explored in HIV research as a means to achieving a functional HIV cure.[5–8] The major barrier to an HIV cure is the presence of latently infected cells (e.g., CD4+ T cells, macrophages and other myeloid lineage cells) that reactivate to produce new virus when antiretroviral therapy (ART) is discontinued or interrupted, making ART an expensive lifelong treatment for people living with HIV.[9,10] Epigenetic changes in the nuclei of latently infected cells harboring the HIV genome may include heterochromatin

formation to compact the chromatin and prevent virus transcription, which can reactivate upon cell activation by an antigen or changes in local inflammatory milieu.[11] Anti-HIV siRNA have been developed to prevent virus reactivation by mimicking this natural latent virus state using a novel "block and lock" approach to control the latent reservoir through blocking virus transcription and locking the genome in a latent state.[4,5,12–15] Two unique siRNA sequences, termed si143 and siPromA, have been developed by Kelleher and co-workers to target highly conserved regions in the non-transcribed 5'LTR promoter of the HIV genome.[5, 7] By binding to its target on the 5'LTR, these siRNAs induce sustained and profound TGS of the virus, switching off virus production, with up to 1000-fold decrease in viral replication lasting several weeks after a single siRNA transfection using commercial transfection agents or nucleofection,[16] or >12 months by matching short hairpin (sh)RNAs delivered by a retroviral construct.[16] *In vivo* humanized mouse model studies also demonstrate virus suppression and protection of CD4+ T cells.[17]

While recombinant viral strategies for the delivery of si/shRNA for PTGS and TGS have led to effective delivery *in vitro* and *in vivo*, viral transduction does not necessarily target resting (non-activated) cells, which constitute the latent HIV reservoir. In addition, safety concerns associated with viral approaches to delivery and cargo limitations (e.g., size, type), have led to research into biocompatible non-viral delivery platforms with potential for development as multifunctional *in vivo* injectable therapeutic carriers. Here we describe the application of poly-L-arginine (PLArg)-terminated multilayered particles and capsules as non-viral platforms for the delivery of siRNA to induce TGS of virus in HIV infection models. The multilayered particles are assembled using layer-by-layer (LbL) deposition of electrostatically interacting PLArg and poly-4-styrene sulfonate (PSS) on a decomposable silica core (template).[18,19] Upon core dissolution, hollow capsules consisting of polymer shell can be obtained. LbL systems have been investigated for the delivery of various cargoes,[20,21] including siRNA (for

PTGS),[22,23] small molecule drugs, proteins, and DNA, and have the advantage over other carriers, such as liposomes and polymer micelles, of being a versatile system with tailorable properties, including size, shape, composition, and degradability.[24,25] In addition, templated LbL systems enable loading of active cargo within the core, embedded within the layers, or adsorbed on the particle surface, as demonstrated for applications including atherosclerosis, cancer therapy, and vaccines.[19,25]

In this work, siPromA was bound electrostatically to PLArg-terminated core-shell particles (837 nm silica core) and hollow shell capsules. While the size of the particles is large for nuclear entry, the PLArg-terminated film allows for effective siRNA deposition and cell uptake that can be adapted to smaller particles (e.g., gold nanoparticle cores) in future studies, particularly *in vivo*.[26,27] We show that PSS/PLArg LbL particles and capsules are able to deliver TGS-inducing siRNA into the nucleus of HIV-infected HeLa T4+ cells, activated primary CD4+ T cells, resting primary CD4+ T cells and monocyte-derived macrophages (MDM). Importantly, studies in HeLaT4+ cells, primary activated CD4+ T cells and MDM showed the siRNA delivered was functional, and induced HIV-1 gene silencing, as determined by reverse transcriptase (RT) and RT-qPCR assays. This study demonstrates particle-mediated nuclear delivery of siRNA for TGS, which has not been reported before.

EXPERIMENTAL SECTION

Materials. Polyethylenimine (PEI; low molecular weight (M_w,)), poly-L-arginine (PLArg M_w>70,000 g mol^{-1}), poly(sodium 4-styrenesulfonate) (PSS, M_w>70,000 g mol^{-1}), Dulbecco's phosphate buffered saline (DPBS), sodium acetate (NaOAc), sodium chloride (NaCl), ethylenediaminetetraacetate (EDTA) and hydrofluoric acid (HF) were purchased from Sigma-Aldrich (St. Louis, MI, USA). Silica particles (0.889 ± 0.003 μm, 5% w/v aqueous solution) were purchased from microParticles GmbH (Berlin, Germany). Alexa Fluor 488 NHS ester,

Alexa Fluor 647 NHS ester, Ultrapure water, Quant-iT RiboGreen RNA assay kit, SYBR Gold nucleic acid stain, alamarBlue reagent, Hoescht and wheat germ agglutinin-Alexa Fluor 488 conjugate (WGA488) were purchased from Thermo Fisher Scientific (Waltham, USA).

Film Assembly on Planar Surface. Quartz crystal microbalance with dissipation monitoring (QCM-D; Q-Sense Biolin Scientific AB, Sweden) was used to follow LbL film assembly and to study siRNA binding onto PLArg-terminated film. The gold QCM-D crystals were cleaned with Piranha solution (one part of 30% H_2O_2 in three parts of H_2SO_4) for 2 min, rinsed three times with Milli-Q water and dried with a gentle stream of nitrogen. *Caution: Piranha solution is highly corrosive. Extreme care should be taken when handling Piranha solution and only small quantities should be prepared.* PEI (2 mg mL^{-1} with 1 M NaCl) was prepared in Milli-Q water. PSS (1 mg mL^{-1} with 0.5 M NaCl) and PLArg (1 mg mL^{-1}) were prepared in 50 mM NaOAc buffer, pH 5.2. PEI was deposited as the first layer to prime multilayer growth, followed by deposition of four PSS/PLArg bilayers. Adsorption of each layer was carried out for 15 min, followed by a series of 5 min washing cycles between deposition steps (two washes with Milli-Q water and two washes with NaOAc after PEI, and three washes with NaOAc after subsequent layers). siRNA (0.5mg mL^{-1} solution in NaOAc) was deposited for 20 min on the [PEI-$(PSS/PLArg)_4$] assembled film, followed by washing with NaOAc. The mass of adsorbed siRNA was calculated using Sauerbrey's equation $\Delta m = -C\Delta f/n$, where the mass sensitivity constant C equals 17.7 ng cm^2 Hz^{-1} for a 5 MHz crystal, Δf is the normalized frequency change (Hz) and n is the number of the harmonic.[28]

Atomic force microscopy (AFM) imaging of PEI-$(PSS/PLArg)_2$ and PEI-$(PSS/PLArg)_2$-siRNA films was carried out with a JPK NanoWizard II BioAFM. Typical scans were performed in tapping mode with MikroMasch silicon cantilevers (NSC/CSC). The roughness of the air-dried films was analyzed using the JPK SPM image processing software (version V.3.3.32).

Particle Preparation. Silica particles (40 μL, 0.05 wt%) were washed three times by centrifugation/resuspension cycles (200 μL of Milli-Q water, 500 *g* for 1.5 min). PEI (200 μL) was incubated with the particles (resuspended in 200 μL Milli-Q water) with mixing in a rotating mixer for 15 min, followed by washing once with Milli-Q water (200 μL) and twice with 50 mM NaOAc (200 μL), which was used in all subsequent washing steps. Particles were then incubated (alternately) with PSS or PLArg (500 μL) for 15 min per layer followed by washing. After deposition of nine layers, i.e., [PEI-(PSS/PLArg)$_4$], particles were resuspended in buffer (100 μL), counted by flow cytometry (Apogee Micro, Apogee Flow Systems, Hertfordshire) and stored at 4 °C until use. ζ-potential measurements were performed in Milli-Q water at 25 °C in folded capillary cells (DTS1070, Malvern Instruments) using a Zetasizer Nano-ZS (Malvern Instruments, United Kingdom).

Capsules were prepared by dissolving the silica core with hydrofluoric acid (HF). Buffered HF (300 μL, 2 M HF in 8 M NH_4F pH 4) was added to PLArg-terminated core-shell particles (40 μL or ~6×10^8 particles in NaOAc) and incubated for 5 min at room temperature. *[Caution! HF is highly toxic. Extreme care should be taken when handling HF solution].* The capsules were pelleted at 4500 *g*, supernatant was removed, and capsules were then washed by centrifugation with Ultrapure water (once) and NaOAc buffer three times to ensure that the HF was fully removed.

To prepare fluorescently labeled particles, PLArg labeled with AF488 or AF647 was used in the seventh layer of the LbL film. PLArg solution (2 mg mL^{-1}) was prepared in 50 mM sodium acetate buffer pH 5.2 and mixed with AF488-NHS (1.75 μL) or AF647-NHS (3.5 μL) (equivalent of 2.8×10^{-4} mmol) and incubated for at least 2 h, with mixing, at room temperature. The free dye was removed by extensive dialysis (MWCO 3.5 kDa) against Milli-Q water over two days. The final product was freeze dried and stored at 4 °C until use.

Particle Imaging. Particles (core-shell, capsules or siRNA-coated) were imaged with a Nikon A1R confocal microscope using 60 × 1.4 NA oil immersion or 40 × 1.2 NA water objectives. Changes in the surface morphology of the silica templates before and after LbL assembly were analyzed by scanning electron microscopy (SEM). Particles (~2×10^6) were deposited on the clean silicon wafer and were washed three times with Milli-Q water over 24 h, allowing the sample to air-dry between washing steps. Images were acquired using a FEI Quanta 200 field emission SEM with 10 kV operation voltage. The thickness of the capsules was analyzed by AFM. Capsules were deposited on a clean glass microscopy slide (~1×10^7 capsules), air-dried for 24 h at room temperature and imaged in tapping mode with a JPK NanoWizard II BioAFM instrument.

Quantification of siRNA Binding. The RiboGreen assay was used to quantify siRNA binding. siRNA solution (20 µL, 3 pmol in 0.2× DPBS) was added to 20 µL particle solutions of varying particle number (1×10^6 to 2×10^7) and incubated for 20 min at room temperature (23 °C), with mixing by vortexing every 5 min. Samples were pelleted then by centrifugation at 600 *g* for 5 min and 10 µL of the supernatant was transferred to a 96-well microplate and mixed with of 1×TE buffer (90 µL). Samples containing only buffer, a particle only control (1×10^6) and a positive control containing siRNA (3 pmol) were also prepared. The RiboGreen assay was performed according to the manufacturer's protocol. Fluorescence measurement was performed with an Infinite M200 microplate reader (Tecan, Switzerland).

Complexation of siRNA was also studied by polyacrylamide gel electrophoresis. Samples with varying number of particles (from 1×10^3 to 1×10^6) in 15 µL NaOAc buffer were mixed with siRNA (15 µL, 3 pmol) and incubated for 20 min at room temperature, followed by addition of nucleic acid loading dye (5 µL). Samples (30 µL) were loaded onto the 10% tris-borate-EDTA (TBE) gel and electrophoresis was carried out for 1 h at 150 V. The gel was

stained with SYBR Gold reagent and imaged using a Bio-Rad ChemiDoc XRS-Imaging System.

Cell Culture. Cell culture reagents were purchased from Gibco™ (Thermo Fisher Scientific, Waltham, USA) unless otherwise specified. HEK293T cells (Invitrogen, Carlsbad, CA) and the HeLa cell line TZM-bl (NIH AIDS Reagent program, Division of AIDS, NIAID, NIH from John C Kappes, Xiaoyun Wu and Tranzyme (Catalogue No. 8129)) were grown in Dulbecco's Modified Eagle Medium (DMEM) supplemented with 10% Fetal Bovine Serum (FBS), 100 U mL^{-1} penicillin and 100 μg mL^{-1} streptomycin (Pen/Strep). HeLa and RAW 264.7 cell lines were cultured in DMEM with GlutaMAX, supplemented with 10% FBS. The HeLa T4+ cell line was grown in the same media with the addition of 200 μg mL^{-1} Geneticin selective antibiotic G418 to only keep cells expressing the stable transduced CD4 Receptor. HUT78 T cell line was grown as suspension cells in Roswell Park Memorial Institute (RPMI) 1640 with 2 mM GlutaMax, 10% FBS and Pen/Strep. All cells were cultured at 37 °C with 5% CO_2.

Cell Viability and Particle Association in Non-infected Cells. Cell viability was assessed using the alamarBlue assay. HeLa, RAW 264.7 and HUT78 cells were seeded at 1×10^5 cells per well in a 96-well microplate (flat-bottom for HeLa and RAW 264.7 cells, round-bottom for HUT78 cells) and incubated overnight. The media was replaced with fresh media (120 μL) and particles and particles-siRNA complexes (30 μL in 0.2× DPBS) were added to cells at particle-to-cell ratios: 50, 200, and 1000 corresponding to 5×10^5, 2×10^6 and 1×10^7 particles per well, respectively. After 24 h incubation at 37 °C, 5% CO_2 in a humidified atmosphere, the alamarBlue assay was performed according to the manufacturer's instructions. HeLa and RAW264.7 were incubated in alamarBlue reagent for 4 h and HUT78 were incubated for 24 h. Plate fluorescence was measured on a Tecan Infinite M200 microplate reader using 560 nm excitation and 590 nm emission wavelengths.

The cell association of particles and capsules complexed with AF647-labeled siRNA was assessed by confocal microscopy. Cells (HeLa, RAW 264.7 and HUT78) were seeded overnight in 8-well chamber slides (Nunc Lab-Tek) at 6×10^4 cells per well in medium (400 μL). The media was replaced with fresh media (370 μL), followed by addition of particles and incubation for 24 h at cell culture conditions. Note that complexation of siRNA with particles and capsules was based on 1.2×10^7 particles per 6 pmol of siRNA in a 30 μL final volume. Before imaging, cells were washed 3 times with DPBS (200 μL; HUT78 were washed by centrifugation/resuspension cycles) and fixed with 4% paraformaldehyde (PFA) for 10 min at room temperature. Nuclei were stained with Hoechst (1 μg mL^{-1}) and cell membranes were stained with WGA488 (5 μg mL^{-1}) for 5 min at room temperature, followed by two washes with DPBS. Images were acquired with a Nikon A1R confocal microscope with a 60× 1.4NA oil immersion objective and analyzed using Fiji software.

Isolation of Primary CD4+ T cells and Monocyte-derived Macrophages. Healthy donors were consented under St Vincent's Hospital ethics #HREC/13/SVH/145. Peripheral blood mononuclear cells (PBMCs) were isolated from fresh blood of healthy donors following informed written consent using Ficoll density gradient. Monocytes were extracted from PBMCs by anti-CD14 magnetic bead positive selection as outlined by the manufacturer's protocol for the anti-CD14 MicroBeads, human (Miltenyi Biotech, Gladbach, Germany) with the exception of using DPBS supplemented with 1% (v/v) human AB serum (hAB) (Merck, Darmstadt, Germany) and 1 mmol L^{-1} EDTA as buffer at 4°C. CD4+ T cells were isolated from the flow through by negative selection using the CD4+ T Cell Isolating Kit, human (Miltenyi Biotech, Gladbach, Germany) following manufacturer's protocol with the buffer change as described for monocyte extraction.

Purified monocytes were cultured into Monocyte-derived-Macrophages (MDMs) by plastic adherence to the tissue culture treated plate for 1 h with RPMI 1640 with 2 mM GlutaMax,

before adding RPMI 1640 with 2 mM GlutaMax supplemented with 20% hAB serum to get to final concentration of 10% hAB. Media was refreshed after 24 h and every 3 days thereafter. MDMs were used for experiments after 7 days of differentiation.

Purified CD4+ T cells were either directly used as resting CD4+ T cells at 1×10^6 cells mL^{-1} in RPMI 1640 with 2 mM GlutaMax and 2% hAB or resuspended at 2.5×10^6 cells mL^{-1} or activated using the T Cell Activation/Expansion Kit, human (Miltenyi Biotech, Gladbach, Germany) following the manufacturer's protocol with the exception of using half the recommended amount of loaded activation beads. Cells were incubated for 48 h at 37 °C, 5% CO_2 before removing the beads as per protocol. Activated CD4+ T cells were cultured at 1×10^6 cells mL^{-1} for experiments.

Plasmids. The lentiviral plasmid psPAX2 was obtained through the NIH AIDS Reagent program, Division of AIDS, NIAID, NIH: psPAX2 (Catalogue No. 11348) from Didier Trono. The lentiviral envelope plasmid VSV-G was kindly donated by A/Prof S.G. Turville. The plasmid pNL4-3 was obtained from the NIH AIDS Reagent Program, Division of AIDS, NIAID, NIH: HIV-1 NL4-3 Infectious Molecular Clone (pNL4-3) (Catalogue No. 114) from Dr. Malcolm Martin. HIV-$1_{NL4.3}$-Δenv-mOrange (NL4.3 virus with 3 stop-codons in the env region and the mOrange inserted into the gag region), HIV-$1_{pBalI\text{-}NL4.3}$ (NL4.3 virus with the envelope region exchanged to the BalI virus envelope sequence) and HIV-$1_{NL4.3}$-IRES-GFP plasmid were modified and kindly donated by A/Prof S.G. Turville.

HIV-1 Virus and Lentivirus Production and Titration. HIV-1_{SF162} was obtained through the NIH AIDS reagent program, Division of AIDS, NIAID from Dr. Jay Levy. HEK293T cell cultures were infected to expand the virus and the supernatant was harvested. During the expansion of HIV-1_{SF162}, the virus encounter mutations in the V3 loop changing its tropism from CCR5 to CXCR4, as previously reported.[29]

HIV-$1_{NL4.3}$ and HIV-$1_{pBalI\text{-}NL4.3}$ were produced by transfecting the virus plasmid with 1X PEI into HEK293T cells. The plasmid was diluted to 10 μg in a solution (500 μL) of tissue culture grade 0.9% (w/v) NaCl (Sigma Aldrich, Missouri, USA), and PEI Max (60 μL) (Polysciences, Warminster, PA) was added dropwise and vortexed for 10 s. The DNA-PEI mix was incubated for 30 min at room temperature and then 7×10^6 trypsinized HEK293T cells were added dropwise to the mixture and incubated for 5 min at room temperature. The mixture was added to a T-75 Flask and cultured in a final volume (10 mL) of DMEM with 10% FBS. The media was replaced at 18 h post transfection. 72 h post-transfection the supernatant was harvested by centrifugal preclearing of viral supernatant at 2500 *g* for 20 min at 4 °C, aliquoted and frozen at −80 °C.

Subsequently generated HIV-1 virus titer was determined on the indicator cell line TZM-bl and the Reed Muench method was used to extrapolate the virus titer.[30] The HIV-$1_{NL4.3}$-IRES-GFP was used with an optimized envelope to infect resting CD4+ T cells. To produce the VSV-G pseudotyped HIV-$1_{NL4.3}$-Δenv-mOrange lentivirus, the PEI transfection method was used. For 7×10^6 cells mL^{-1} HEK293T cells, psPAX2 plasmid (4 μg), VSV-G envelope plasmid (1 μg) and HIV-$1_{NL4.3}$-Δenv-mOrange plasmid (4 μg) were added to PBS (0.5 mL) and incubated with 1× PEI (60 μL) for 10 min. After adding the cells to the PEI-plasmid mix and incubating for another 5 min, the cells were seeded in a T-75 cell culture flask and incubated for 72 h at 37 °C, 5% CO_2. Viral supernatant was harvested by centrifugal preclearing at 2500 *g* for 20 min at 4 °C, aliquoted and frozen at −80 °C. Titration of VSV-G envelope pseudotyped, mOrange expressing HIV-$1_{NL4.3}$-Δenv was performed by infecting HEK293T cells in multiple dilutions. 72 h post infection cells were harvested and fixed in 0.5% PFA and expression of mOrange was checked using the flow cytometry.

Infection of Cells with HIV. Infection of any cells was performed at multiplicity of infection (MOI) of 1 at time of seeding. HeLa T4+ and HUT78 T cells were infected with HIV-1_{SF162};

activated CD4+ T cells were infected with HIV-$1_{NL4.3}$ by spinoculation at 200 *g* for 2 h at 37 °C. MDMs were infected with HIV-$1_{pBalI-NL4.3}$ by spinoculation at 200 *g* for 1 h at 37 °C. Infection of cell lines, primary activated CD4+ T cells and MDMs for imaging was performed using a VSV-G envelope pseudotyped, mOrange expressing HIV-$1_{NL4.3-\Delta env}$. No spinoculation was needed. Cell lines and MDMs were infected for 4 days and activated CD4+ T cells were infected for 3 days prior to commencing experiments. Resting CD4+ T cells were infected with an optimized HIV-$1_{NL4.3-IRES-GFP}$ and used for experiments 5 days post infection.

Reverse Transcriptase Assay. Supernatant of infected cells was collected on multiple days post LbL particle/capsule siRNA delivery. Supernatant samples were stored at −80 °C until the RT assay was performed on all samples as previously described.[31]

RNA Extraction and Real Time Quantitative PCR. Cells were harvested at specified timepoint, centrifuged at 300 *g* for 5 min, supernatant removed, and cell pellet frozen at −80 °C. RNA extraction was performed using Monarch® total RNA Miniprep Kit (New England BioLabs, Massachusetts, USA) following manufacturer's protocol. RNA was adjusted to 10 ng μL^{-1}. Real-time qPCR was performed using the Luna® Universal One-Step RT-qPCR Kit as per the manufacturer's protocol (E3005) and the CFX96 detection system (New England BioLabs, Massachusetts, USA). Primers included:

β2 microglobulin (B2M)-Fwd: GGACTGGTCTTTCTATCTCTTGT;

B2M-Rev:ACCTCCATGATGCTGCTTAC;

HIV-$1_{NL4.3}$ Gag-Fwd: GTTTTCAGCATTATCAGAAGGAGCCAC;

Gag-Rev: CTTGGTTCTCTCATCTGGCCTG. All plates contained β2 microglobulin (B2M) as a housekeeping gene for normalization and a HIV gene standard.

Imaging and Image Analysis. Imaging was performed on the DeltaVision ELITE Image Restoration Microscope (Applied Precision/Olympus) using the 60× oil immersion lens with 1.58 NA. The CoolSnap QE camera (Photometrics) was used with the dichroic 1 filter to detect

nuclei stained with NucBlue with DAPI, GFP with FITC, mOrange-labelled virus with TRITC and siRNA-AlexaFluor647 with Cy5. Cells were seeded in either a 96 well or 384 well microplate (Ibidi, Wisconsin, USA) and cells were stained with NucBlue Live Cell Stain (Thermo Fisher Scientific, Waltham, USA) and fixed with 4% PFA (Electron Microscopy Sciences, Pennsylvania, USA) for 12 min at RT prior to storage in PBS at 4 °C for imaging at a later timepoint. Gain was set to 2. Z-stacks (up to 50) of ~0.5 μm per stack were obtained to enable generation of a 3D cell using the SoftWoRx 3D Volume Viewer tool. Deconvolution of images was performed using the SoftWoRx software prior to analysis. To define siRNA as a nuclear event the arbitrary line intensity profile and 3D Volume Viewer was used. The arbitrary line was drawn through the region of interest and the signal intensity of each channel was obtained. If the area denoting the nuclear signal included a peak for the siRNA signal, they were considered as potentially nuclear. Verification was done using the 3D Volume viewer to produce a 3D projection of the nucleus from all optical sections. This 3D projection was used to exclude siRNA in nuclear pockets. Final confirmation of entry was determined by rendering of the cell into nuclear and cytoplasmic compartments, with only siRNA completely enclosed in the nucleus being confirmed nuclear events.

Statistical Analysis. All statistical analyzes were performed using GraphPad Prism 9 (La Jolla, CA). To determine the statistical difference of means among various groups, data was analyzed with one-way or two-way ANOVA test with the appropriate multiple comparisons test. A p value of <0.05 was considered statistically significant.

RESULTS AND DISCUSSION

Production and Characterization of LbL Particles and Capsules. The design of particles for siRNA delivery typically requires a cationic component that can complex negatively charged siRNA, protect it from degradation by serum nucleases, mediate transport across the

cell membrane and promote endosomal escape into the cytoplasm, where it can block translation of mRNA into proteins via PTGS. For TGS, the siRNA must also enter the nucleus to allow binding to its target sequence in the genome and to suppress gene transcription (Figure 1). Poly-L-arginine is a cationic polypeptide that has been used to enhance the intracellular translocation of various cargoes via a mechanism that resembles the action of arginine-rich HIV-derived transactivator of transcription (Tat) — the first identified cell-penetrating peptide.[32, 33] In addition, nuclear localization signals that transport proteins to the cell nucleus are often arginine-rich, which may provide an additional benefit for the use PLArg for enhanced nuclear translocation of nucleus-bound siRNA.[34,35] In this study, PLArg was used in the assembly of multilayered particles and capsules to facilitate complexation with negatively charged siRNA by electrostatic interactions. Microcapsules containing PLArg have been previously reported to deliver and release loaded cargo upon degradation by intracellular proteases *in vitro*.[36, 37]

Multilayered particles and capsules were prepared by LbL assembly of PLArg and anionic PSS on spherical silica templates (Figure 2a). PSS is a highly biocompatible, FDA-approved material for applications in the gastrointestinal tract and has a demonstrated ability to form stable multilayers with PLArg.[37] LbL assembly of PLArg and PSS and subsequent siRNA binding to terminal PLArg layer were first studied on a planar surface using quartz crystal microgravimetry with dissipation (QCM-D), which confirmed multilayer build up (Figure S1).

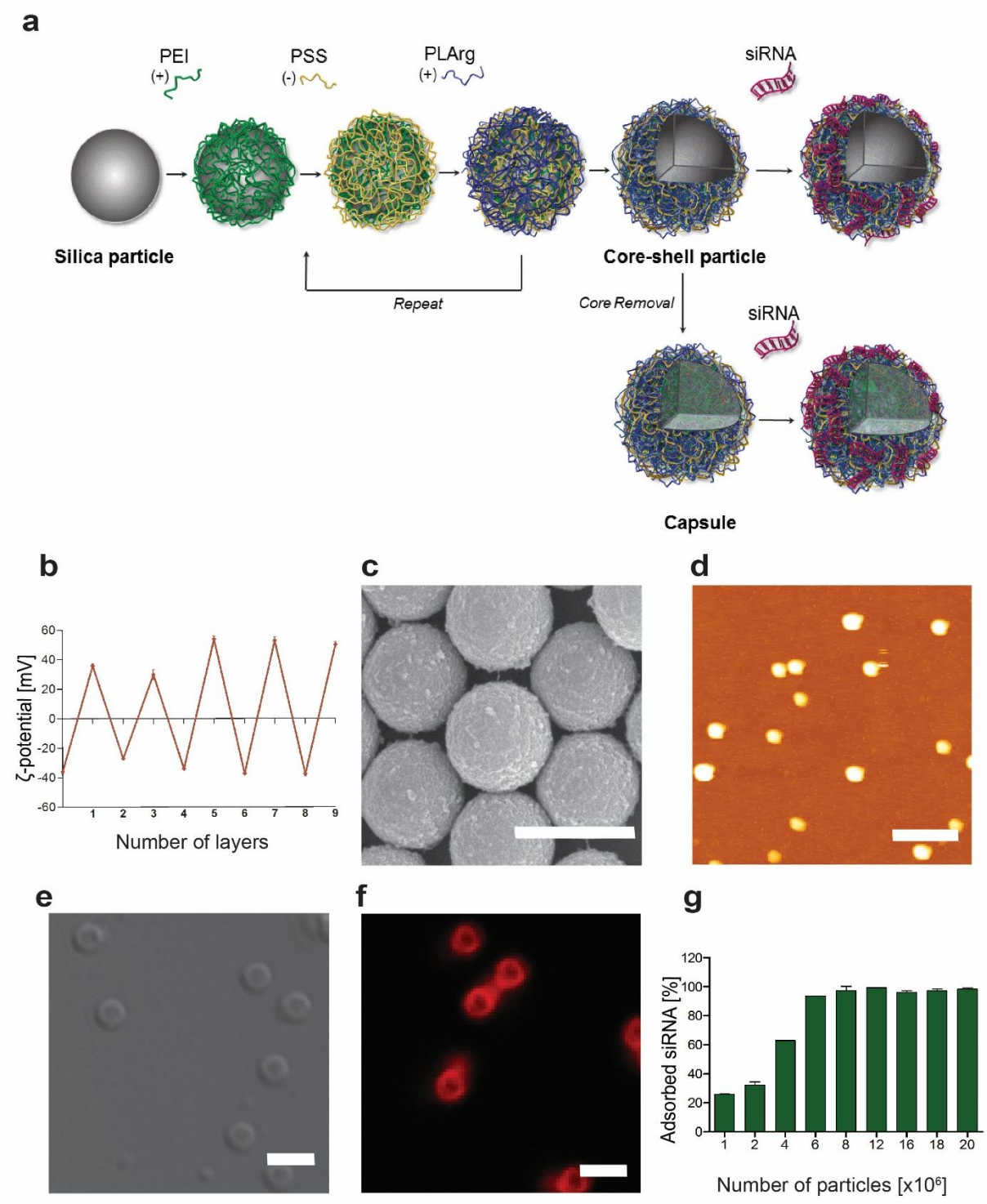

Figure 2. Preparation and characterization of PSS/PLArg particles and capsules. (a) LbL particles were prepared by deposition of anionic PSS and cationic PLArg on spherical PEI-coated silica templates to form a multilayer shell comprising PEI-$(PSS/PLArg)_4$. Upon dissolution of the silica core, hollow capsules are formed. siRNA is complexed by PLArg-terminated core-shell particles or capsules via electrostatic interactions between positively

charged amine groups in PLArg and negatively charged phosphate groups in siRNA. (b). Multilayer build up was monitored by zeta potential measurements; layer 1 is PEI, layers 2, 4, 6 and 8 correspond to the deposition of PSS; layers 3, 5, 7 and 9 correspond to the deposition of PLArg. (c) SEM image of silica particles coated with a PEI-$(PSS/PLArg)_4$ film (core-shell particles). Scale bar is 1 μm. (d) AFM image of hollow capsules after silica removal. Scale bar is 5 μm. (e) Differential interference contrast (DIC) microscopy image of hollow capsules and (f) fluorescence image of capsules complexed with AF647-labeled siRNA. Scale bars are 2 μm. (g) Optimization of siRNA complexation on PLArg-terminated particles using the RiboGreen assay.

Multilayer build up was adapted to spherical templates to prepare core-shell particles on silica templates and subsequently, hollow capsules after template removal. Silica particles (837 nm in diameter) were first coated with PEI to prime the multilayer growth followed by four PSS/PLArg bilayers for a film structure of PEI-$(PSS/PLArg)_4$. The assembly process was followed by microelectrophoresis, which determines the ζ-potential of the particles and is related to the particle surface charge. The pattern of ζ-potential reversal from negative to positive is indicative of multilayer film formation on a spherical template (Figure 2b).[38] Scanning electron microscopy (SEM) was also used to confirm film formation, which revealed a rough surface morphology after deposition of a PEI-$(PSS/PLArg)_4$ film compared with bare silica particles (Figures 2c, S2a, and S2b). Shell thickness was determined using SEM by comparing the diameter of the particles before and after film assembly. By measuring the diameters of 50 particles using the imaging software Fiji, particle diameter was determined to increase from 846 ± 32 nm for the bare silica template to 905 ± 32 nm after LbL film assembly. The increase in diameter indicates the formation of a ~41 nm thick film on the particle surface after deposition of nine polyelectrolyte layers [PEI-$(PSS/PLArg)_4$]. By using fluorescently labeled PLArg within the film [PEI-$(PSS/PLArg)_2$(PSS/PLArg-AF488) (PSS/PLArg)],

confocal microscopy could be used to image the film of core-shell particles (Figure S2c), and to confirm binding of AF647-labeled siRNA on non-fluorescent PLArg-terminated core-shell particles (Figure S2).

Silica core removal resulted in hollow microcapsules, as confirmed using atomic force microscopy (AFM) and differential interference contrast (DIC) microscopy (Figure 2d, e). While silica is a highly biocompatible drug delivery material,[39] hollow capsules that result from core removal can have distinct mechanical properties (i.e., flexibility) that can influence particle interaction with the biointerface.[40] Images of capsules in the air-dried state showed collapsed and monodispersed structures with a 45 nm shell thickness, as determined by AFM height analysis (Figure S3). DIC microscopy of the capsules in a hydrated state (in solution) showed uniform capsules having similar size as core-shell particles (~900 nm in diameter) (Figure 2e). The adsorption of AF647-labeled siRNA to the microcapsules, likely from the electrostatic interaction of siRNA with PLArg, was confirmed by confocal microscopy (Figure 2f), and showed fluorescence of the capsule shell after washing. The presence of siRNA resulted in the decrease in the ζ-potential of the capsules from 50 ± 5 mV to -6 ± 4 mV. This is consistent with siRNA binding to PLArg-terminated core-shell particles in which the ζ-potential decreased from 51 ± 5 mV to 7 ± 4 mV after siRNA binding (Figure S4). The increase in surface film roughness because of siRNA binding was also confirmed by AFM (Figure S5).

The amount of siRNA bound to the particles was quantified by RiboGreen RNA quantification assay (Figure 2g), which determined complete complexation of 3 pmol siRNA by 6×10^6 particles. This was confirmed by the disappearance of the unbound siRNA band at this ratio by polyacrylamide gel electrophoresis (Figure S6). An estimated coverage of 266 ng siRNA per cm^2 is obtained, which is consistent with the siRNA surface coverage obtained from QCM-D data (255 ng per cm^2) (Figure S1). Since, in principle, only one siRNA molecule is needed to bind the target genomic sequence to induce epigenetic silencing, 266 ng siRNA per

cm^2 or roughly equivalent to 2.7×10^5 siRNA molecules per particle presents an excess amount of siRNA accessible to the cell upon particle internalization.

Cell Viability is Unaffected by LbL Particle Treatment *in Vitro*. The cytotoxicity of LbL core-shell particles and capsules was tested in non-virus infected HeLa, HUT78 and RAW 264.7 cell lines using the alamarBlue viability assay. LbL particles and capsules, with or without bound siRNA, were incubated with cells at particles-to-cell ratio of 50, 200 and 1000, to reflect conditions used in later experiments in infected cultures. At least 80% viability was observed in all tested conditions up to particle-to-cell ratio 1000 for all tested cell lines (i.e., HeLa, HUT78 and RAW 264.7) (Figure S7). For HUT78 cells incubated with capsules, an increase in cell death is observed as the capsule-to-cell ratio increases and when capsules have surface-bound siRNA. However, this is not observed in the other cell lines studied and may be a cell-specific trend that warrants further investigation beyond the present study. Nevertheless, the generally high cell viability across the different cells and particles indicates the highly biocompatible nature of the PSS/PLArg LbL particles *in vitro*. Efficient cellular uptake of siRNA coated LbL core-shell particles and capsules after 24 h incubation with Hela, HUT78 and Raw 264.7 cells was demonstrated by confocal microscopy (Figure S8).

LbL Capsule Delivery of siPromA to the Nuclei of HeLa T4+ Cells. Having established that siRNA-coated LbL particles/capsules are internalized by non-infected cells within 24 h, we proceeded to investigate siRNA entry into the nucleus in HIV-infected cells. For successful epigenetic silencing to occur, siRNA targeting the HIV promoter (i.e., siPromA) needs to be transported into the nucleus and interact with its complementary sequence within the genome. The release of siRNA from the particle and siRNA entry into the nucleus of infected cells was analyzed in the HeLa T4+ cell line, as well as primary activated and resting CD4+ T cells and MDMs, both of which represent the predominant primary cell types that harbor the latent HIV reservoir.

HeLa T4+ cells were seeded and infected for 4 days prior to addition of siRNA-coated capsules. For imaging purposes, cells were infected with a fluorescently labeled (mOrange) HIV pseudovirus and were fixed 48 h post-siRNA-capsule treatment. For functional assays, cells were infected with HIV-1_{SF162} and were analyzed 16 days post siRNA-capsule treatment (Figure 3a). Note that treatment and infection of cells was different for every cell type, with day 0 representing the day the siRNA-loaded capsules were added for all cell types (Table S1).

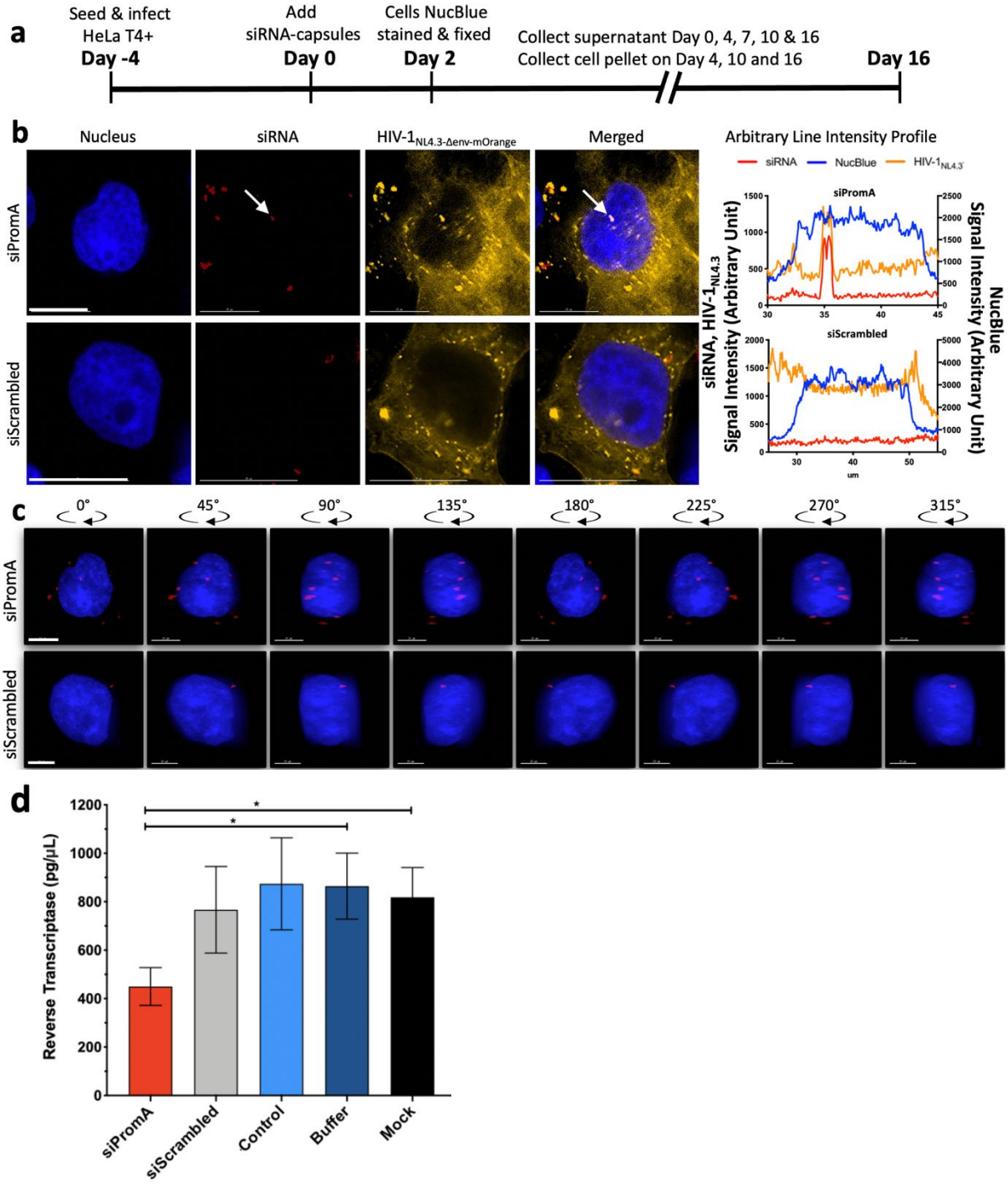

Figure 3. Nuclear delivery and functional characterization of siRNA capsule-treated HeLa T4+ cells. (a) HeLa T4+ cells were infected with VSV-G envelope pseudotyped, mOrange expressing HIV-$1_{NL4.3}$-Δenv for imaging (b-c) or with HIV-1_{SF162} for the reverse transcriptase (RT) assay (d) for 4 days. In (b) infected cells were transfected with AF647-

labeled siRNA (red) complexed by PLArg-terminated LbL capsules and incubated for 48 h prior to fixation and deconvolution microscopy. Nuclei were stained with NucBlue (blue). (b) Upper panels depict nuclear siPromA localization and lower panels show cytoplasmic location of the specificity control, siScrambled. Each panel contains single channel images for nucleus (blue), siRNA-AF647 (red), HIV-$1_{NL4.3}$-Δenv-mOrange (orange), a merged image and an arbitrary line signal intensity profile. A representative siPromA inside the nucleus is indicated by the white arrow. Scale bars 15 μm. (c) siRNA localization was confirmed by the generation of a 3D volume viewer. Upper and lower panels display 45° rotations of nuclear siPromA and cytoplasmic siScrambled, respectively. The 3D viewer shows nuclei (blue) and siRNA (red). Scale bars 10 μm. In (d), infected cells were treated with siRNA-capsules and RT expression was measured in duplicate over a 16-day time course post particle addition ($n = 4$). Data shown is at day 16. * $p < 0.03$ with a Wilcoxon test.

Confirmation of siRNA localization was performed by deconvolution microscopy and the use of the arbitrary line intensity profile, showing entry into the nucleus if the AF647-siRNA fluorescence peak is within the area of the nuclear signal (Figure 3b). While confocal microscopy is typically used for studying particle internalization, deconvolution algorithms can also enable analysis of internalization inside cells, as previously reported.[5,41,42] 3D volume views of deconvoluted images were also used to confirm the localization of siRNA (i.e., inside or outside the nucleus), by compiling the multiple z-stack images and rotating the nucleus at 45° angles (Figure 3c). Image analysis of 500 cells indicated the localization of siPromA inside the nucleus occurred in 2.4% of infected HeLa T4+ cells, compared to siScrambled (i.e., non-targeted sequence), which was not observed inside the nucleus of any infected cells. The low number of nuclear occurrences of siPromA in HeLa T4+ cells indicates the transfection efficiency of the siRNA delivery via the LbL particles is also low, however the cultures are also heavily infected with HIV and therefore not optimally functioning. Additionally, the

trafficking of HIV in the cell and the trafficking of siRNA both utilize the actin cytoskeleton, as we have described for siRNA,[43] suggesting that again due to HIV infection the nuclear delivery of siRNA may be decreased. Avenues to enhance the nuclear delivery of siRNA involve co-delivery of essential proteins involved in the epigenetic silencing process, which is currently under investigation. We postulate the siScrambled RNA was not observed inside the cell nucleus due to the highly sequence specific nature of RNAi via TGS and lack of the complementary gene sequence in the cell genome. In contrast, siPromA targeting the HIV promoter region is translocated to the nucleus in virus-infected cells. Although the selective nuclear entry mechanism of epigenetic silencing siRNA is still to be determined in mammalian cells, the process in yeast is reported to involve an Argonaute siRNA chaperone (ARC)-licensing complex. We speculate a similar complex is present in mammalian cells, as we have previously reported this observation of selective nuclear entry in HIV-infected cell lines where promoter-targeted siRNA was delivered using Lipofectamine transfection.[7,13,15,43] Interestingly, particle-delivered siRNA that did not enter the nucleus did not appear to be observed at specific locations in the cytoplasm.

LbL Capsule-Delivered siPromA Silences Gene Expression in HeLa T4+ Cells *in Vitro*. To determine whether functional silencing was achieved by capsule-delivered siPromA, we performed an HIV-1 reverse transcriptase (RT) assay to quantify levels of the virus RT protein over 16 days. Successful silencing is expected to show reduced RT protein in infected, treated cell cultures compared to control cultures. Infected HeLa T4+ cells showed significantly reduced levels of RT (~50% less) following capsule-mediated delivery of siPromA at day 16, compared to mock control (HIV infection alone) and buffer alone cultures (Figure 3d). The reduced viral protein levels in capsule-delivered siPromA cultures compared to controls demonstrate that functional silencing of HIV-1 infection was achieved in HeLa T4+ cells.

LbL Capsule Delivery of siPromA to the Nuclei of Primary Activated CD4+ T Cells. Following the confirmation of siPromA entry into the nucleus of the infected HeLa T4+ cell line and functional virus suppression, we next investigated capsule-mediated delivery of siPromA in primary human cell types relevant to the HIV latent reservoir. We extracted CD4+ T cells via negative magnetic bead selection from fresh blood and then activated the cells for 48 h (Figure 4a) using anti-biotin MACSiBead particles loaded with biotinylated human CD2, CD3, and CD28 antibodies to mimic antigen-presenting cells and activate resting CD4+ T cells. Activation is required to enable uptake of virus via endocytosis, which does not occur in resting CD4+ T cells isolated from blood. Infection of activated CD4+ T cells using a VSV-G pseudotyped HIV-$1_{NL4.3}$-Δenv-mOrange virus resulted in ~60% of cells being infected at day 3, as determined by detecting mOrange-expressing cells. LbL capsules were complexed with siRNA and added at a particle-to-cell ratio of 80 for a 48 h incubation (Table S1). From analysis of deconvolution microscopy images, we observed successful delivery of siPromA to the nucleus (Figure 4b) of 12% HIV-infected activated CD4+ T cells. Localization of siPromA inside the nucleus and siScrambled outside the nucleus is shown in fluorescence images and was further confirmed using the arbitrary line intensity profile. Representative cells are shown for activated CD4+ T cells with siPromA and siScrambled in a 3D volume viewer rotation, which confirmed siPromA nuclear localization and siScrambled cytoplasmic localization (Figure 4c).

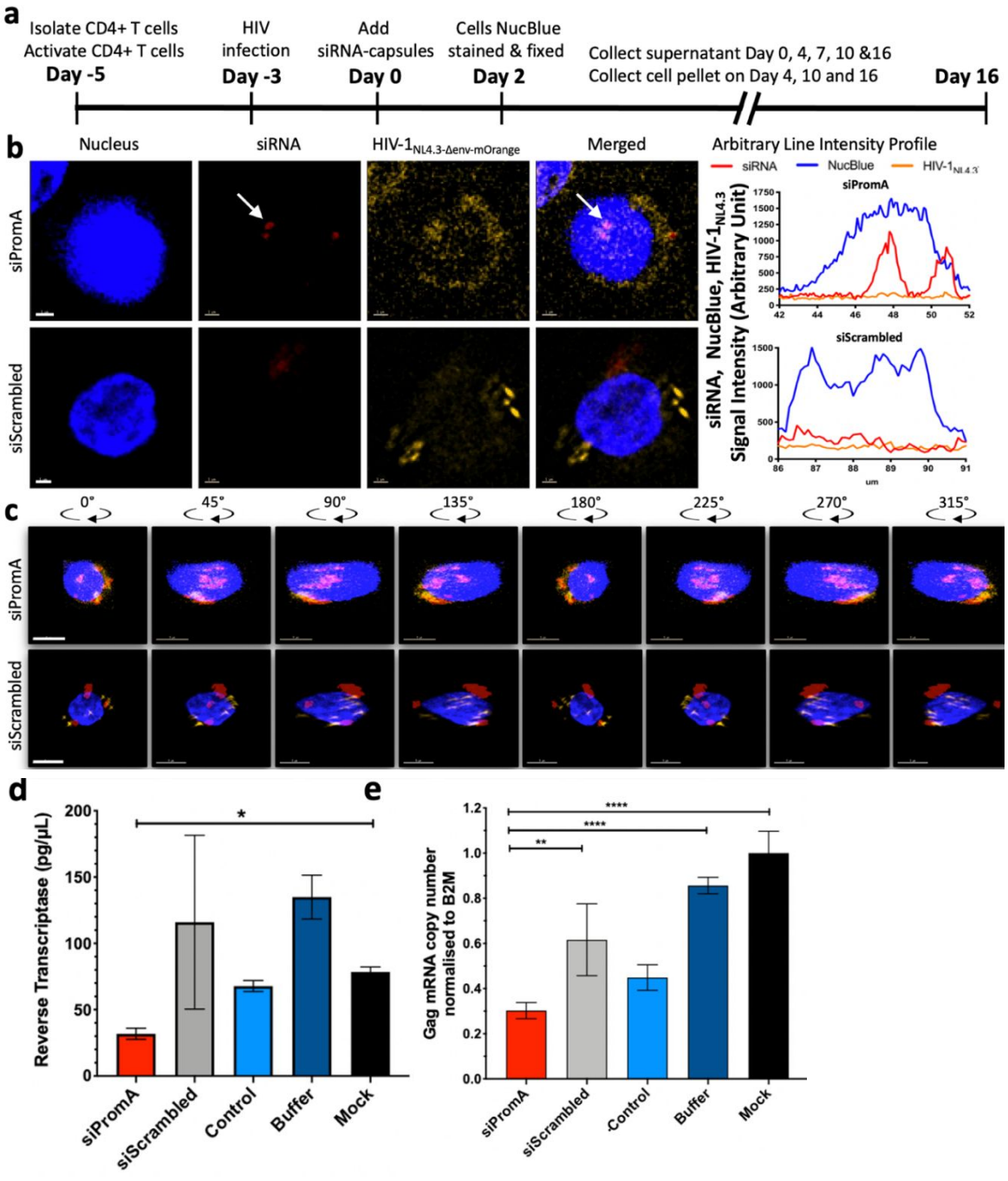

Figure 4. Nuclear delivery and functional characterization of siRNA-capsule in primary activated CD4+ T cells. (a) CD4+ T cells were isolated from fresh blood, activated for 48 h and infected with VSV-G envelope pseudotyped, mOrange expressing HIV-$1_{NL4.3}$-Δenv for imaging (b-c) and with HIV-$1_{NL4.3}$ for functional assays (d-e) for 4 days, followed by the transfection of AF647-labeled siRNA (red) complexed by PLArg-terminated LbL capsules and incubated for 48 h for imaging and 16 days for functional assays. Cells were fixed and imaging

was performed on the Deltavision Elite microscope. Nuclei were stained with NucBlue (blue). (b) Upper panels depict nuclear siPromA localization and lower panels show the cytoplasmic location of the specificity control siScrambled. Each panel contains single channel images for NucBlue (blue), siRNA-AF647 (red), HIV-$1_{NL4.3}$-Δenv-m-Orange (orange), a merged image and an arbitrary line signal intensity profile. A representative siPromA inside the nucleus is indicated by the white arrow. Scale bars 1 μm. (c) siRNA localization was confirmed by the generation of a 3D volume viewer. Upper and lower panels display 45° rotations of nuclear siPromA and cytoplasmic siScrambled, respectively. The 3D viewer shows nuclei (blue) and siRNA (red). Scale bars 5 μm. Image b-c are representative from 3 donors. In (d), infected cells were treated with siRNA-capsules and the RT concentration was measured in duplicate over a 16-day time course post particle addition (donor 1 data shown). Data shown is at day 16. * p = 0.011 with a Brown-Forsythe and Welch ANOVA, Dunnett's multiple comparisons test. (e) real time qPCR was performed to quantify HIV-1 *gag* mRNA copy number relative to beta-2 microglobulin (B2M) housekeeping gene on day 4, 10 and 16 post particle addition. Data shown is Day 16 for Donor 1. ** p= 0.006, **** p <0.0001. Ordinary one-way ANOVA multiple comparisons.

LbL Capsule Delivered siPromA Silences Gene Expression in Primary Activated CD4+ T Cells *in Vitro*. Functional gene silencing induced by LbL capsule delivered siPromA in activated CD4+ T cells was assessed by measuring RT protein levels and virus *gag* mRNA levels by real time qPCR (Figures 4d and 4e). Particle-to-cell ratio was increased to 200 for functional studies in primary cells. A significant decrease in virus RT protein was measured in the supernatant of capsule delivered siPromA treated cultures for Donor 1 compared to controls at 16 days post-particle addition (Figure 4d). The decrease in virus RT in cultures other than siPromA-treated cultures is due to cell death of activated primary CD4+ T cells, which had

been in culture for 15 days post-extraction from whole blood and 12 days since activation (Figure 4a). Data for Donors 2 and 3 highlight the variability between donors, although the capsule delivered siPromA treated cultures typically show the lowest levels of virus RT protein (Figure S9). Real time qPCR was performed for CD4+ T cells on day 4, 10 and 16 for Donor 1 (Figure 4e) and Donor 3 (Figure S9), comparing the amount of virus *gag* mRNA between cultures after normalization to the housekeeping gene beta-2 microglobulin (B2M). The decrease in *gag* mRNA copy number for all donors confirm functional silencing of virus gene expression is induced by LbL capsule-delivered siPromA.

LbL Capsule Delivery of siPromA to the Nuclei of Primary Resting CD4+ T Cells. Analysis of primary resting CD4+ T cells was performed by infecting resting CD4+ T cells with an HIV-$1_{BalI\text{-}NL4.3}$-GFP reporter virus for 5 days after isolation from whole blood prior to addition of particle-siRNA suspension and fixation of cells for imaging 48 h later (Figure 5a). Infection of resting CD4+ T cells was performed using a system that ensures CD4+ T cells keep their resting state and are not activated during the process of infection, which achieved ~30% infection as determined by GFP detection.[44] As resting CD4+ T cells are by definition 'resting', it was therefore not possible to perform the functional assays (as in previous cell types) to detect production of virus RNA or protein which usually required cellular activation. Instead, we used deconvolution microscopy to analyze successful delivery of fluorescently labeled siRNA into the nucleus of virus-infected resting CD4+ T cells. LbL capsule delivered siPromA was observed inside the nucleus of ~15% of infected resting CD4+ T cells, while capsule delivered siScrambled was not observed inside the nucleus of infected resting CD4+ T cells. Image analysis was performed as previously described, in combination with the arbitrary line intensity profile and 3D Volume viewer, to examine localization of siRNA (Figures 5b and 5c). SiRNA loaded capsules are observed surrounding resting CD4+ T cells in both cultures, but siRNA was only found inside the nucleus of infected cells in the siPromA culture

48 h post particle addition. Delivery of gene therapy agents to resting CD4+ T cells is one major challenge in HIV cure research.[4,45,46] This is because resting CD4+ T cells harbor latent HIV that can reactive when the cell is activated.[47,48] Delivery of siPromA to the nucleus of infected resting CD4+ T cells *in vitro* using the LbL capsule system is therefore a major advance, indicating the possibility of using particle-based delivery systems to successful delivery gene therapy agents to HIV harboring resting cells. Despite the low rate of siPromA nuclear delivery (15%), this was achieved without active targeting (e.g., conjugating an antibody to the particle), which may be necessary to facilitate delivery to the ~10^6 cells estimated to harbor latent virus in the human body.

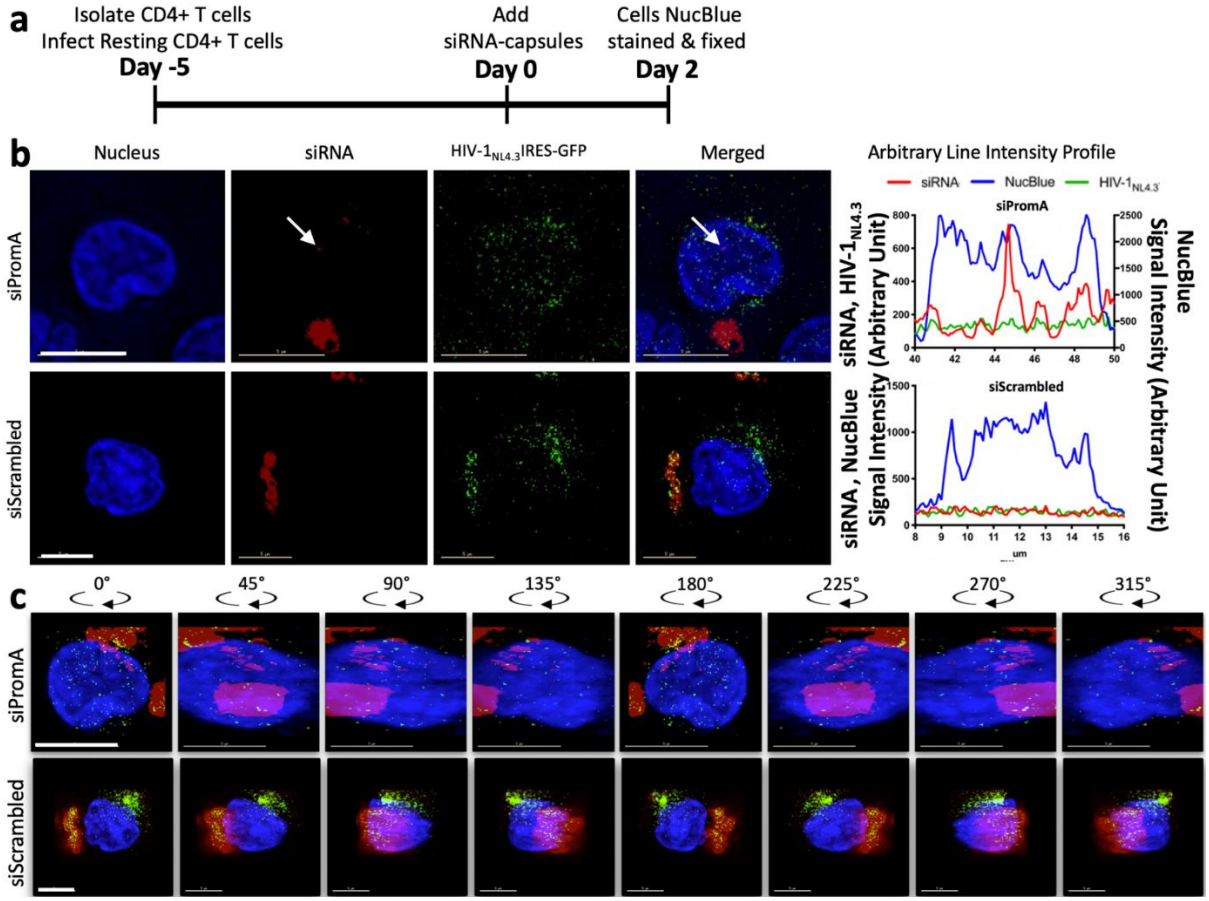

Figure 5. Nuclear delivery of siRNA-capsules in primary resting cells. (**a**) CD4+ T cells were isolated from fresh blood and infected with optimized HIV-$1_{NL4.3\text{-}IRESGFP}$ for 5 days, followed by the transfection of AF647-labeled siRNA (red) complexed by PLArg-terminated capsules and incubated for 48 h. Cells were fixed and imaging was performed by deconvolution

microscopy. Nucleus was stained with NucBlue (blue). (b) Upper panels depict nuclear siPromA localization and lower panels show the cytoplasmic location of the specificity control siScrambled. Each panel contains single channel images for NucBlue (blue), siRNA-AF647 (red), HIV-$1_{NL4.3\text{-}IRESGFP}$ (green), a merged image and an arbitrary line signal intensity profile. A representative siPromA inside the nucleus is indicated by the white arrow. Scale bars 5 μm. (c) siRNA localization was confirmed by the generation of a 3D volume viewer. Upper and lower panels display 45° rotations of nuclear siPromA and cytoplasmic siScrambled, respectively. The 3D viewer shows nuclei (blue), siRNA (red) and HIV-$1_{NL4.3\text{-}IRESGFP}$ (green). Scale bar 5 μm.

LbL Particle Delivery of siPromA to the Nuclei of Monocyte-Derived Macrophages. As macrophages also represent a potential HIV-1 latent reservoir cell type,[49,50] we examined the LbL particle delivery system in primary human MDMs. Monocytes were extracted from three healthy donors and differentiated into MDMs over 7 days. HIV-1 infection of MDMs was performed using VSV-G envelope pseudotyped, mOrange expressing HIV-$1_{NL4.3}$-Δenv for imaging studies and HIV-$1_{BalI\text{-}NL4.3}$ for functional studies for 5 days prior to particle-siRNA addition. Cell cultures for imaging were fixed 48 h post capsule-siRNA addition, whereas cultures for functional assays were followed over 16 days (Figure 6a). Due to the high amount of siRNA fluorescence detected in LbL capsule delivered siPromA in MDMs, we were unable to definitively analyze nuclear entry or localization, although we observed efficient uptake of LbL capsules into MDMs, which is consistent with the phagocytotic characteristics of macrophages. We therefore used the LbL core-shell particles with the intact silica core at the same particle:siRNA and particle:cell ratios as previously used (Table S1) to assess delivery of siRNA to MDMs. Successful uptake of LbL core-shell particles into cells was observed particularly for siScrambled, with MDMs internalizing numerous particles into the cytoplasm of the representative cell shown (Figure 6b). Nuclear localized siPromA was observed in ~12%

of all analyzed infected cells over 3 donors, as determined by image analysis, arbitrary line intensity profile and the 3D volume viewer (Figures 6b and 6c). As observed in CD4+ T cells, the proportion of MDMs with nuclear localization of siPromA was low.

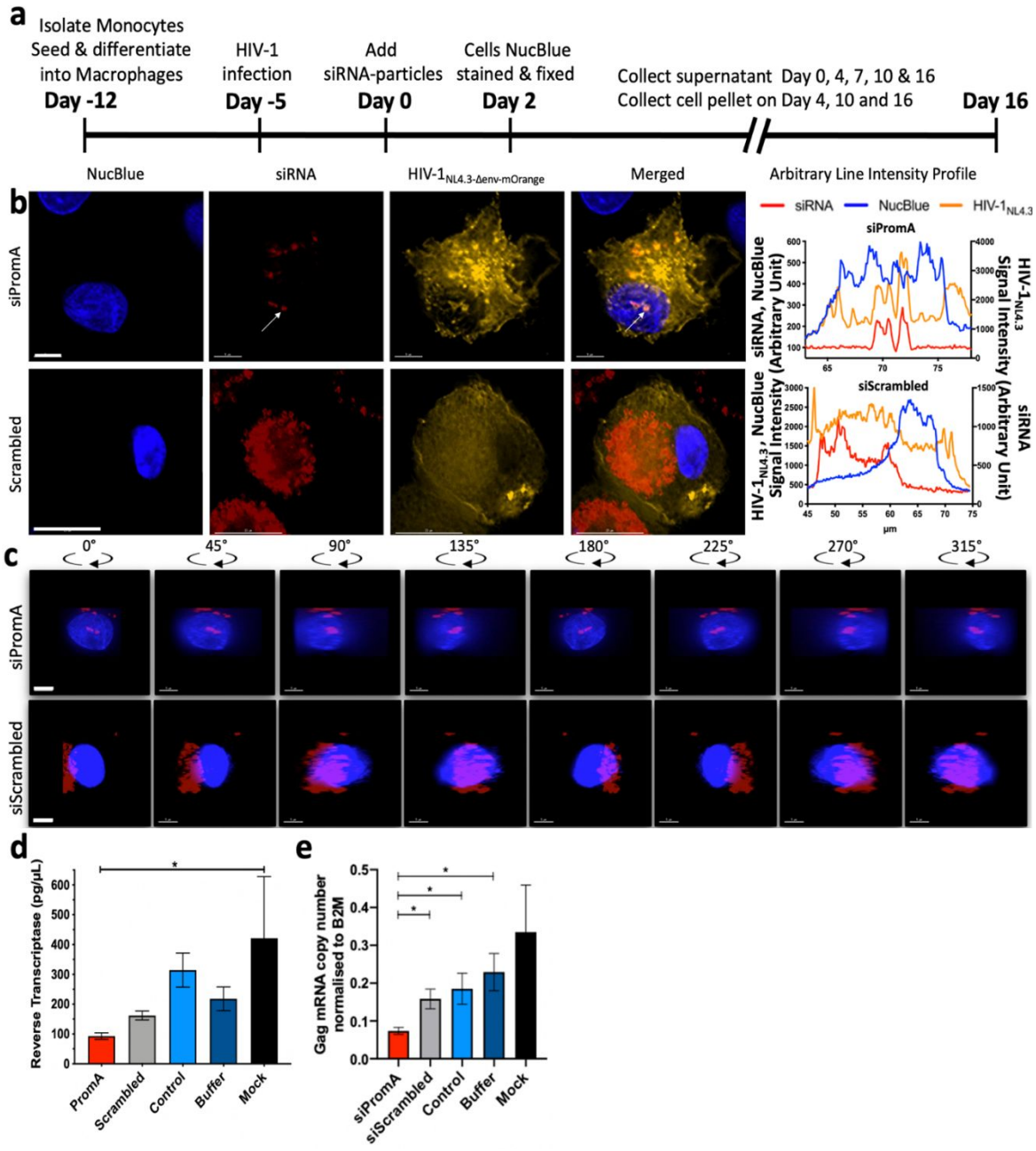

Figure 6. siRNA delivery into HIV-1 infected primary MDMs. (a) MDMs were isolated from fresh blood, differentiated for 7 days and infected with VSV-G envelope pseudotyped, mOrange expressing HIV-$1_{NL4.3\text{-}\Delta env}$ for imaging (b-c) and with HIV-$1_{BaII\text{-}NL4.3}$ for functional assays (d-e) for 4 days, followed by the transfection of AF647-labeled siRNA (red) complexed

by PLArg-terminated core-shell particles and incubated for 48 h. Cells were fixed and imaging was performed by deconvolution microscopy. Nucleus was stained with NucBlue (blue). (b) Upper panels depict nuclear siPromA localization and lower panels show the cytoplasmic location of the specificity control siScrambled. Each panel contains single channel images for NucBlue (blue), siRNA-AF647 (red), HIV-$1_{NL4.3}$-Δenv-mOrange (orange), a merged image and an arbitrary line signal intensity profile. A representative siPromA inside the nucleus is indicated by the white arrow. Scale bars 5 µm upper panels, 15 µm lower panels. (c) siRNA localization was confirmed by the generation of a 3D volume viewer. Upper and lower panels display 45° rotations of nuclear siPromA and cytoplasmic siScrambled, respectively. The 3D viewer shows nuclei (blue) and siRNA (red). Scale bar 5 µm. (b-c) images shown are representative for 3 Donors. (d) Quantification of viral RT was performed on days 4, 7, 10, 13 and 16 post particle addition. Day 16 Donor 1 data shown. * p = 0.02. Ordinary one-way ANOVA with Dunnett's multiple comparisons test. (e) real time qPCR was performed for HIV-1 *gag* mRNA relative to a housekeeping gene (B2M) on day 4, 10 and 16 post particle addition. Donor 1 data at day 16 is shown. * p <0.036. Unpaired t test, Welch's correction.

LbL Particle Delivered siPromA Silences Gene Expression in MDMs *in Vitro*. Functional assays measuring virus RT and viral *gag* mRNA were performed for all three donors and confirmed functionality in MDMs, with significantly reduced RT protein (~75% less) and viral *gag* RNA levels (~50% less) in particle-siPromA treated MDM cultures compared to controls (Figures 6d, 6e and S10). These data demonstrate that despite the larger diameter (900 nm) of the particles, delivery of the anti-HIV nuclei acid siPromA via the LbL particle platform can achieve functional gene silencing of HIV-1. Future work will focus on improving the nuclear entry of siRNA using smaller particles that are more readily internalized by T cells[51] and with enhanced endosomal escape capacity to pave the way for *in vivo* studies in HIV animal models.[52]

CONCLUSIONS

While care of patients with HIV-1 infection has been transformed by ART, continuous lifelong therapy is required from the time of diagnosis. This study has developed an LbL capsule for delivery of siRNA mediating transcriptional gene silencing of HIV-1 in the nucleus of HIV-infected cells. The LbL capsule system mediated the delivery of siPromA into the nucleus to the gene promoter site and induced a decrease in virus RNA and protein levels. The LbL capsule/particle-delivered siPromA specific gene silencing was reported in HeLa T4+ cell line, primary CD4+ T cells and primary monocyte-derived macrophages, of which the primary cells are key targets of the HIV latent reservoir. The diverse locations of the HIV latent reservoir, which include the gastrointestinal tract, central nervous system, blood, lymph nodes, and other organs, including lungs and skin, mean that identifying a single particle system with the appropriate size, surface properties, loading and intracellular delivery capacity to target the reservoir is challenging. This work, although using particles that may readily be cleared after intravenous injection in vivo, provides the basis for further research into non-viral particle platforms for nuclei-targeted siRNA delivery to achieve epigenetic silencing of genes implicated in disease.

ASSOCIATED CONTENT

Supporting Information. QCM-D data of multilayer film formation; SEM of silica core before and after film coating; fluorescence images of capsules and siRNA-capsule complexes; AFM analysis of capsules; ζ-potential of particles and capsules before and after siRNA adsorption; AFM image of LbL film after siRNA adsorption; PAGE analysis of siRNA binding; cell viability of particles in non-infected cells; confocal microscopy images of siRNA delivery into non-infected cell lines; table of LbL core-shell particle/capsule to siRNA ratio for different cell types; functional characterization of capsule-siRNA in primary activated CD4 T cells and MDMs. This material is available free of charge via the Internet at http://pubs.acs.org.

AUTHOR INFORMATION

Corresponding Author

* cahlenstiel@kirby.unsw.edu.au

*ccortez@unimelb.edu.au

Author Contributions

The manuscript was written through contributions of all authors. All authors have given approval to the final version of the manuscript. ‡These authors contributed equally.

ACKNOWLEDGMENT

This research was supported by the Australian National Health and Medical Research Council (NHMRC; Program Grant GNT1149990) and the Australian Research Council Centre of Excellence in Convergent Bio-Nano Science and Technology (project number CE140100036). F.C. acknowledges the award of an NHMRC Senior Principal Research Fellowship (GNT1135806). The authors thank Dr. Gyengwon Yun and Dr. Qi-Zhi Zhong for the AFM imaging, and Dr. Zhixing Lin for the SEM analysis.

REFERENCES

1. Kelleher, A. D.; Cortez-Jugo, C.; Cavalieri, F.; Qu, Y.; Glanville, A. R.; Caruso, F.; Symonds, G.; Ahlenstiel, C. L. RNAi therapeutics: an antiviral strategy for human infections. *Curr. Opin. Pharmacol.* **2020**, *54*, 121–129.

2. Dong, Y.; Siegwart, D. J.; Anderson, D. G. Strategies, design, and chemistry in siRNA delivery systems. *Adv. Drug Delivery Rev.* **2019**, *144*, 133–147.

3. Suzuki, K.; Ahlenstiel, C.; Marks, K.; Kelleher, A. D. Promoter targeting RNAs: Unexpected contributors to the control of HIV-1 transcription. *Mol. Ther. Nucleic Acids* **2015**, *4*, e222.

4. Ahlenstiel, C. L.; Symonds, G.; Kent, S. J.; Kelleher, A. D. Block and lock HIV cure strategies to control the latent reservoir. *Front. Cell. Infect. Microbiol.* **2020**, *10*, 424.

5. Ahlenstiel, C.; Mendez, C.; Lim, S. T.; Marks, K.; Turville, S.; Cooper, D. A.; Kelleher, A. D.; Suzuki, K. Novel RNA duplex locks HIV-1 in a latent state via chromatin-mediated transcriptional silencing. *Mol. Ther. Nucleic Acids* **2015**, *4*, e261.

6. Ahlenstiel, C. L.; Suzuki, K.; Marks, K.; Symonds, G. P.; Kelleher, A. D. Controlling HIV-1: Non-coding rna gene therapy approaches to a functional cure. *Front. Immunol.* **2015**, *6*, 474.

7. Mendez, C.; Ledger, S.; Petoumenos, K.; Ahlenstiel, C.; Kelleher, A. D. RNA-induced epigenetic silencing inhibits HIV-1 reactivation from latency. *Retrovirology* **2018**, *15*, 67.

8. Klemm, V.; Mitchell, J.; Cortez-Jugo, C.; Cavalieri, F.; Symonds, G.; Caruso, F.; Kelleher, A. D.; Ahlenstiel, C. Achieving HIV-1 control through RNA-directed gene regulation. *Genes* **2016**, *7*, 119.

9. Finzi, D.; Blankson, J.; Siliciano, J. D.; Margolick, J. B.; Chadwick, K.; Pierson, T.; Smith, K.; Lisziewicz, J.; Lori, F.; Flexner, C.; Quinn, T. C.; Chaisson, R. E.; Rosenberg, E.; Walker, B.; Gange, S.; Gallant, J.; Siliciano, R. F. Latent infection of CD4+ T cells provides a mechanism for lifelong persistence of HIV-1, even in patients on effective combination therapy. *Nat. Med.* **1999**, *5*, 512–517.

10. Ho, Y. C.; Shan, L.; Hosmane, N. N.; Wang, J.; Laskey, S. B.; Rosenbloom, D. I.; Lai, J.; Blankson, J. N.; Siliciano, J. D.; Siliciano, R. F. Replication-competent noninduced proviruses in the latent reservoir increase barrier to HIV-1 cure. *Cell* **2013**, *155*, 540–551.

11. Siliciano, R. F.; Greene, W. C. HIV latency. *Cold Spring Harbor Perspect. Med.* **2011**, *1*, a007096.

12. Suzuki, K.; Hattori, S.; Marks, K.; Ahlenstiel, C.; Maeda, Y.; Ishida, T.; Millington, M.; Boyd, M.; Symonds, G.; Cooper, D. A.; Okada, S.; Kelleher, A. D. Promoter targeting shRNA suppresses HIV-1 infection *in vivo* through transcriptional gene silencing. *Mol. Ther. Nucleic Acids* **2013**, *2*, e137.

13. Suzuki, K.; Ishida, T.; Yamagishi, M.; Ahlenstiel, C.; Swaminathan, S.; Marks, K.; Murray, D.; McCartney, E. M.; Beard, M. R.; Alexander, M.; Purcell, D. F.; Cooper, D. A.; Watanabe, T.; Kelleher, A. D. Transcriptional gene silencing of HIV-1 through promoter targeted RNA is highly specific. *RNA Biol.* **2011**, *8*, 1035–1046.

14. Suzuki, K.; Juelich, T.; Lim, H.; Ishida, T.; Watanebe, T.; Cooper, D. A.; Rao, S.; Kelleher, A. D. Closed chromatin architecture is induced by an RNA duplex targeting the HIV-1 promoter region. *J. Biol. Chem.* **2008**, *283*, 23353–23363.

15. Suzuki, K.; Shijuuku, T.; Fukamachi, T.; Zaunders, J.; Guillemin, G.; Cooper, D.; Kelleher, A. Prolonged transcriptional silencing and CpG methylation induced by siRNAs targeted to the HIV-1 promoter region. *J. RNAi Gene Silencing* **2005**, *1*, 66–78.

16. Yamagishi, M.; Ishida, T.; Miyake, A.; Cooper, D. A.; Kelleher, A. D.; Suzuki, K.; Watanabe, T. Retroviral delivery of promoter-targeted shRNA induces long-term silencing of HIV-1 transcription. *Microbes Infect.* **2009**, *11*, 500–508.

17. Tsukamoto, T.; Kariya, R.; Marks, K.; Hattori, S.; Ahlenstiel, C. L.; Symonds, G.; Okada, S.; Kelleher, A. D. Transcriptional gene silencing limits CXCR4-associated depletion of bone marrow CD34+ cells in HIV-1 infection. Erratum. *AIDS* **2018**, *32*, 2857–2858.

18. Caruso, F.; Caruso, R. A.; Mohwald, H. Nanoengineering of inorganic and hybrid hollow spheres by colloidal templating. *Science* **1998**, *282*, 1111–1114.

19. Richardson, J. J.; Bjornmalm, M.; Caruso, F. Multilayer assembly. Technology-driven layer-by-layer assembly of nanofilms. *Science* **2015**, *348*, aaa2491.

20. Becker, A. L.; Johnston, A. P.; Caruso, F. Layer-by-layer-assembled capsules and films for therapeutic delivery. *Small* **2010**, *6*, 1836–52.

21. Linnik, D. S.; Tarakanchikova, Y. V.; Zyuzin, M. V.; Lepik, K. V.; Aerts, J. L.; Sukhorukov, G.; Timin, A. S. Layer-by-Layer technique as a versatile tool for gene delivery applications. *Expert Opin. Drug Delivery* **2021**, *18*, 1047–1066.

22. Becker, A. L.; Orlotti, N. I.; Folini, M.; Cavalieri, F.; Zelikin, A. N.; Johnston, A. P.; Zaffaroni, N.; Caruso, F. Redox-active polymer microcapsules for the delivery of a survivin-specific siRNA in prostate cancer cells. *ACS Nano* **2011**, *5*, 1335–1344.

23. Boehnke, N.; Correa, S.; Hao, L.; Wang, W.; Straehla, J. P.; Bhatia, S. N.; Hammond, P. T. Theranostic Layer-by-layer nanoparticles for simultaneous tumor detection and gene silencing. *Angew. Chem. Int. Ed.* **2020**, *59*, 2776–2783.

24. Elbakry, A.; Zaky, A.; Liebl, R.; Rachel, R.; Goepferich, A.; Breunig, M. Layer-by-layer assembled gold nanoparticles for siRNA delivery. *Nano Lett.* **2009**, *9*, 2059–2064.

25. Richardson, J. J.; Cui, J.; Bjornmalm, M.; Braunger, J. A.; Ejima, H.; Caruso, F. Innovation in layer-by-layer assembly. *Chem. Rev.* **2016**, *116*, 14828–14867.

26. Wurster, E. C.; Elbakry, A.; Gopferich, A.; Breunig, M. Layer-by-layer assembled gold nanoparticles for the delivery of nucleic acids. *Methods Mol. Biol.* **2013**, *948*, 171–82.

27. Yan, Y.; Such, G. K.; Johnston, A. P.; Lomas, H.; Caruso, F. Toward therapeutic delivery with layer-by-layer engineered particles. *ACS Nano* **2011**, *5*, 4252–4257.

28. Sauerbrey, G. Use of quartz vibration for weighing thin films on a microbalance. *J. Phys.* **1959**, *155*, 206–222.

29. Kiselyeva, Y.; Nedellec, R.; Ramos, A.; Pastore, C.; Margolis, L. B.; Mosier, D. E. Evolution of CXCR4-using human immunodeficiency virus type 1 SF162 is associated with two unique envelope mutations. *J. Virol.* **2007**, *81*, 3657–3661.

30. Reed, L. J. M., H. A simple method of estimating fifty percent endpoints. *Am. J. Epidemiol.* **1938**, *44*, 189–198.

31. Suzuki, K.; Craddock, B. P.; Okamoto, N.; Kano, T.; Steigbigel, R. T. Poly A-linked colorimetric microtiter plate assay for HIV reverse transcriptase. *J. Virol. Methods* **1993**, *44*, 189–98.

32. Frankel, A. D.; Pabo, C. O. Cellular uptake of the tat protein from human immunodeficiency virus. *Cell* **1988**, *55*, 1189–1193.

33. Holowka, E. P.; Sun, V. Z.; Kamei, D. T.; Deming, T. J. Polyarginine segments in block copolypeptides drive both vesicular assembly and intracellular delivery. *Nat. Mater.* **2007**, *6*, 52–57.

34. Nakase, I.; Noguchi, K.; Aoki, A.; Takatani-Nakase, T.; Fujii, I.; Futaki, S. Arginine-rich cell-penetrating peptide-modified extracellular vesicles for active macropinocytosis induction and efficient intracellular delivery. *Sci. Rep.* **2017**, *7*, 1991.

35. Wang, Y. H.; Hou, Y. W.; Lee, H. J. An intracellular delivery method for siRNA by an arginine-rich peptide. *J. Biochem. Biophys. Methods* **2007**, *70*, 579–586.

36. Rivera-Gil, P.; De Koker, S.; De Geest, B. G.; Parak, W. J. Intracellular processing of proteins mediated by biodegradable polyelectrolyte capsules. *Nano Lett.* **2009**, *9*, 4398–4402.

37. Czuba-Wojnilowicz, E.; Viventi, S.; Howden, S. E.; Maksour, S.; Hulme, A. E.; Cortez-Jugo, C.; Dottori, M.; Caruso, F. Particle-mediated delivery of frataxin plasmid to a human sensory neuronal model of Friedreich's ataxia. *Biomater. Sci.* **2020**, *8*, 2398–2403.

38. Caruso, F. L., H.; Donath, E.; Möhwald, H. Investigation of electrostatic interactions in polyelectrolyte multilayer films: binding of anionic fluorescent probes to layers assembled onto colloids. *Macromolecules* **1999**, *32*, 2317–2328.

39. Manzano, M. V.-R., M. Mesoporous silica nanoparticles for drug delivery. *Adv. Funct. Mater.* **2020**, *30*, 1902634.

40. Chen, X.; Cui, J.; Ping, Y.; Suma, T.; Cavalieri, F.; Besford, Q. A.; Chen, G.; Braunger, J. A.; Caruso, F. Probing cell internalisation mechanics with polymer capsules. *Nanoscale* **2016**, *8*, 17096–17101.

41. Yan, Y.; Lai, Z. W.; Goode, R. J.; Cui, J.; Bacic, T.; Kamphuis, M. M.; Nice, E. C.; Caruso, F. Particles on the move: intracellular trafficking and asymmetric mitotic partitioning of nanoporous polymer particles. *ACS Nano* **2013**, *7*, 5558–5567.

42. Izquierdo-Useros, N.; Naranjo-Gómez, M.; Archer, J.; Hatch, S. C.; Erkizia, I.; Blanco, J.; Borràs, F. E.; Puertas, M. C.; Connor, J. H.; Fernández-Figueras, M. T.; Moore, L. Capture and transfer of HIV-1 particles by mature dendritic cells converges with the exosome-dissemination pathway. *Blood* **2009**, *113*, 2732–2741.

43. Ahlenstiel, C. L.; Lim, H. G.; Cooper, D. A.; Ishida, T.; Kelleher, A. D.; Suzuki, K. Direct evidence of nuclear Argonaute distribution during transcriptional silencing links the actin cytoskeleton to nuclear RNAi machinery in human cells. *Nucleic Acids Res.* **2012**, *40*, 1579–1595.

44. Fichter, C.; Aggarwal, A.; Wong, A. K. H.; McAllery, S.; Mathivanan, V.; Hao, B.; MacRae, H.; Churchill, M. J.; Gorry, P. R.; Roche, M.; Gray, L. R.; Turville, S. Modular Lentiviral Vectors for Highly Efficient Transgene Expression in Resting Immune Cells. *Viruses* **2021**, *13*, 1170.

45. Ahlenstiel, C. L.; Turville, S. G. Delivery of gene therapy to resting immune cells for an HIV cure. *Curr. Opin. HIV AIDS* **2019**, *14*, 129–136.

46. Geng, X.; Doitsh, G.; Yang, Z.; Galloway, N. L.; Greene, W. C. Efficient delivery of lentiviral vectors into resting human CD4 T cells. *Gene. Ther.* **2016**, *23*, 320–322.

47. Chomont, N.; El-Far, M.; Ancuta, P.; Trautmann, L.; Procopio, F. A.; Yassine-Diab, B.; Boucher, G.; Boulassel, M. R.; Ghattas, G.; Brenchley, J. M.; Schacker, T. W.; Hill, B. J.; Douek, D. C.; Routy, J. P.; Haddad, E. K.; Sekaly, R. P. HIV reservoir size and persistence are driven by T cell survival and homeostatic proliferation. *Nat. Med.* **2009**, *15*, 893–900.

48. Churchill, M. J.; Deeks, S. G.; Margolis, D. M.; Siliciano, R. F.; Swanstrom, R. HIV reservoirs: what, where and how to target them. *Nat. Rev. Microbiol.* **2016**, *14*, 55–60.

49. Orenstein, J. M.; Fox, C.; Wahl, S. M. Macrophages as a source of HIV during opportunistic infections. *Science* **1997**, *276*, 1857–1861.

50. Wong, M. E.; Jaworowski, A.; Hearps, A. C. The HIV reservoir in monocytes and macrophages. *Front. Immunol.* **2019**, *10*, 1435.

51. Cevaal, P. M.; Ali, A.; Czuba-Wojnilowicz, E.; Symons, J.; Lewin, S. R.; Cortez-Jugo, C.; Caruso, F. *In vivo* T cell-targeting nanoparticle drug delivery systems: Considerations for rational design. *ACS Nano* **2021**, *15*, 3736–3753.

52. Burke, B. P.; Levin, B. R.; Zhang, J.; Sahakyan, A.; Boyer, J.; Carroll, M. V.; Colon, J. C.; Keech, N.; Rezek, V.; Bristol, G.; Eggers, E.; Cortado, R.; Boyd, M. P.; Impey, H.; Shimizu, S.; Lowe, E. L.; Ringpis, G. E.; Kim, S. G.; Vatakis, D. N.; Breton, L. R.; Bartlett, J. S.; Chen, I. S.; Kitchen, S. G.; An, D. S.; Symonds, G. P. Engineering cellular resistance to HIV-1 infection *in vivo* using a dual therapeutic lentiviral vector. *Mol. Ther. Nucleic Acids* **2015**, *4*, e236.

Table of Contents Graphic